Mapping of Nuclear Export Signals and domains mediating aggregation of NBR1

Morten Svendsen Næss, Molecular Cancer Research Group, Institute of Medical Biology, UIT – the Arctic University of Norway

Supervisors: Postdoctoral Research Fellow Steingrim Svenning, Associate Professor Trond Lamark and Professor Terje Johansen

Abstract

Autophagy is a conserved catabolic pathway for the lysosomal degradation of cytoplasmic components. Autophagy can be both selective and unselective. Selective autophagy receptor proteins are involved in mediating the degradation of specific substrates. Among these receptors we find the evolutionary related proteins p62 and NBR1, which are both involved in autophagic degradation of different ubiquitinated substrates. The p62 protein is known to shuttle between the nucleus and cytoplasm dependent on nuclear localization (NLS) and nuclear export sequences (NES). Here, we find that NBR1 harbors two active NES motifs. We also find that the subcellular distribution of NBR1 is dependent on its aggregation status and we map the location of the different domains responsible for aggregation of NBR1.

Introduction

Autophagy is a generalized term for the mechanistic process that delivers cytoplasmic substrates to the lysosome for degradation [1]. Three separate autophagy routes are now recognized, where microautophagy and Chaperone-mediated Autophagy are lesser known pathways involving more or less direct translocation of the substrate across the lysosomal membrane [2]. The third pathway, macroautophagy, is the most well studied and considered the "quintessential" autophagy pathway. Macroautophagy is defined by the formation of a double-membrane structure, known as the phagophore, that envelopes the target substrate and forms a closed vesicle called the autophagosome [3]. The molecular machinery of autophagy has been extensively characterized, in large part based on studies in yeast [4]. The process relies on a core set of AuTophaGy-proteins (ATG) that cooperates to build the autophagosome, as well as other protein complexes involved in initiating the phagophore-formation [5] (Fig. 1).

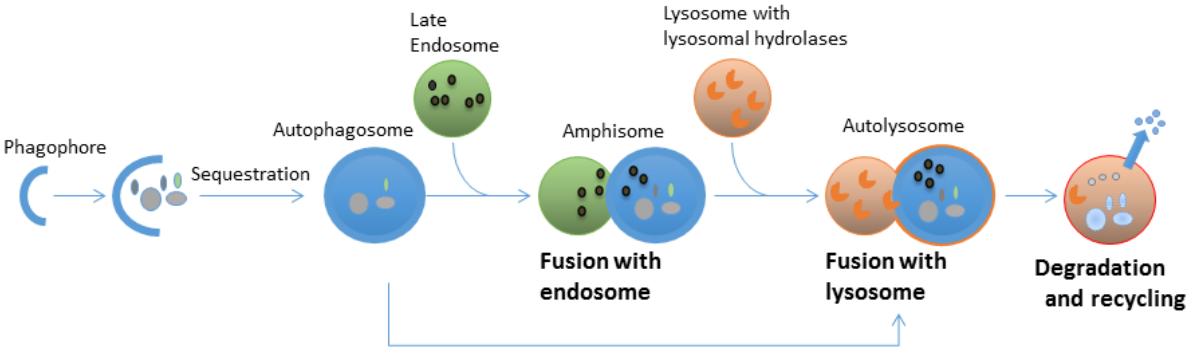

Figure 1. Macroautophagy involves the sequestration of cytoplasmic content into autophagosomes and the subsequent lysosomal degradation of the sequestered material. A double membrane, crescent shaped isolation membrane, or phagophore, forms first and cytoplasmic material is sequestered into the closed autophagosome. The autophagosome fuses either directly with the lysosome to form an autolysosome, or may fuse first with a late endosome, which subsequently fuses with a lysosome. In the autolysosome the inner membrane of the autophagosome and the content are degraded, and building blocks are recycled back to the cytoplasm.

Macroautophagy has likely evolved as a non-selective response to starvation, commonly referred to as bulk autophagy, which acts in freeing nutrients to sustain catabolic processes. However, autophagy can also be selective, and requires specific proteins that aids in recognizing the substrate to be degraded. These proteins are called autophagy receptor proteins and share the common feature of being able to bind simultaneously to a substrate and ATG8 family proteins [6] (Fig. 2). ATG8 family proteins are intrinsically linked to the autophagosome via a phosphatidylethanolamine moiety covalent attached to their C terminus, and as such provides a scaffold to connect the substrate to the autophagosome. The first mammalian autophagy receptor to be characterized was p62/SQSTM1(sequestosome-1) [7]. Based on the functional features of p62, a family of newly characterized receptors have been coined Sequestosome-1-like receptors (SLRs) [8].

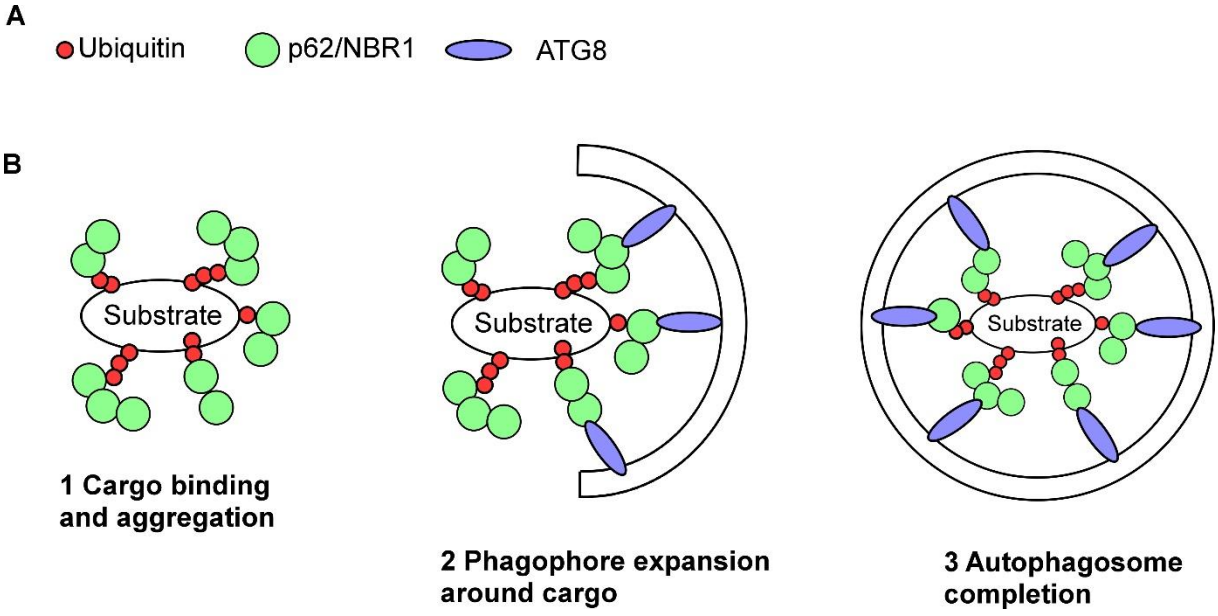

Figure 2. Selective autophagy mediated by receptor proteins. A) Overview of proteins. **B**) Substrates to be degraded by selective autophagy are commonly marked by chains of a small protein called ubiquitin. The selective autophagy receptors, represented here by p62 and NBR1, recognize and bind the ubiquitin chains on the substrate and through homo-dimerization creates an aggregate. When the size of the aggregate has reached a critical mass, it will serve as a nucleation site for the formation of a phagophore, which connects to the substrate through the binding between p62/NBR1 and ATG8. The completed autophagosome fuses to a lysosome where the content is degraded and biomolecules are released back to the cytosol for reuse.

NBR1

The Neighbor of BRCA1 gene 1 (NBR1) in humans is a 966 amino acid (aa) long protein that acts as a selective cargo receptor for autophagy [9, 10] [11] (Fig. 3). NBR1 has several functional domains and has several interaction partners (Fig. 3). Among these, NBR1 interacts with its phylogenetically younger brother p62 via its N-terminal Phox and Bem1p (PB1) domain [12]. Whereas mammals have both NBR1 and p62 genes, most intervertebrates have only p62 after losing NBR1, while many protists and plants have NBR1 only [13] [14]. In addition to sharing a PB1 region, NBR1 and p62 both have a Zink finger like domain (ZZ), LC3-interacting motifs (LIRs) and a C-terminal ubiquitin-associated (UBA) domain that binds ubiquitinated cargo (Fig. 3) [9].

NBR1 interacts with LC3/ATG8 via LIR1 (aa 727-738), a central part of the selective autophagy process as it links the ubiquitinated cargo to the phagophore [9, 10]. LC3 is a mammalian homologue to ATG8 in yeast cells [15]. It is also known that the first coiled coil

region (CC1, aa 288-239) is responsible for homo-dimerization [16]. NBR1 is together with p62 both well-known aggrephagy receptors for selective autophagy, meaning they themselves promote aggregation [11]. At present, we still do not know the true function of the Zink finger domain (aa 211-256), the second coil coiled domain (CC2, aa 693-728) and the two globular domains (Glob1, aa 389-478 and Glob2, aa 497-579). Another domain of unknown function is the FW-domain, which is named based on four conserved tryptophan [14]. The FW-domain is the most conserved feature of NBR1 across phyla, and is therefore used to identify NBR1 [17]. In addition, NBR1 harbors a C-terminal amphipathic alpha helix (AH) which has been shown to bind negatively charged lipids in-vitro, and is indispensable for NBR1s role in Pexophagy [18] [19]. The C-terminal region containing the AH-and UBA-domain is also considered crucial for the aggregating properties of NBR1.

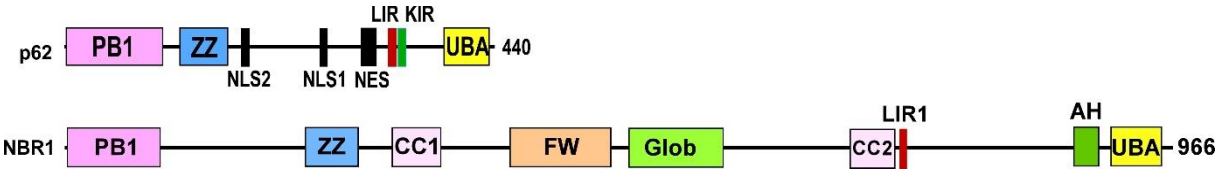

Figure 3. Domain architecture of NBR1 and p62. Schematic representation of protein domains and motifs in the functionally related autophagy receptor proteins p62 and NBR1.

Previous work from our group has shown that p62 exhibits nucleocytoplasmic shuttling, and although p62 is found in ubiquitin-enriched nuclear aggregates associated with certain pathological states, the exact role of p62s involvement in the nucleus has not been established [20, 21].

Nuclear location signals (NLS) and nuclear export signals (NES) are important for shuttling larger proteins between the nucleus and the cytoplasm. Regulation is complex, and the interplay between import and export is strictly regulated to ensure the correct subcellular localization in different conditions. Small proteins pass freely through the nuclear pore complex, while proteins larger than ~ 20-40 kDa in mass, or ~ 5 nanometer, are assisted when passing the nuclear membrane [22]. Due to its 107-kDa size, NBR1 requires NLS and NES to shuttle between the nucleus and the cytoplasm. The consensus sequences for NES reads: Φ x $_{2\text{-}3}$ Φ x $_{2\text{-}3}$ Φ x Φ, where Φ is either hydrophobic amino acid Leucine (L), Isoleucine (I), Valine (V), Phenylalanine (F) or Methionine (M), and x is any amino acid. Hydrophobic amino acids probably bind to a hydrophobic pocket on the outer surface of the transport protein Exportin1

(Chromosomal Maintenance 1, CRM1) [23]. CRM1 is part of a family of exportins and importins, the karyopherins, all contributing to the nuclear pore complex.

NBR1 is an enigmatic protein, and we look into the individual domains, which can provide links to other proteins and consequently aid in understanding the function of NBR1. Our primary aim of this investigation was to map potential NES sequences in NBR1. Second, we sought to find the regions required for aggregation of NBR1.

Materials and Methods

We used recombinant DNA technology to make various cDNA expression constructs of NBR1. We created DNA constructs in entry vectors, verified them by DNA sequencing and transferred them to expression vectors using the Invitrogen Gateway® system. All constructs had an N-terminal tag of enhanced green fluorescent protein (EGFP) to enable visualization of the expressed proteins. The tagged constructs, with various sequences of NBR1, were transiently transfected into mammalian cells (HeLa or Hek293) and analyzed by confocal fluorescence microscopy. NBR1 D50R mutants lack the ability to bind p62, and deletion constructs with this mutation were therefore preferred when assaying cytoplasmic aggregation [12]. We used the pRev1.4-GFP assay system to place putative NES sequence between the nuclear bound Rev protein from HIV and GFP. In some experiments, the nuclear export inhibitor Leptomycin B (LMB) was included. LMB is a fungal metabolite that blocks nuclear export by binding competitively to CRM1 inside the nucleus [23]. Two different nuclear markers were used, DAPI and mCherry Histone3. We also applied antibodies to identify endogenous expression of NBR1.

Plasmids. Plasmids used in this study are listed in Table 1. All plasmids have been made by conventional restriction enzyme-based cloning and by use of the Gateway recombination system (Invitrogen). Gateway LR reactions were performed as described in the Gateway cloning technology instruction manual (Invitrogen). Oligonucleotides for mutagenesis, PCR, and DNA sequencing reactions were obtained from Invitrogen and Sigma. All plasmid constructs were verified by restriction digestion and/or DNA sequencing (BigDye, Applied Biosystems).

Cell culture and immunolabeling. Cells were grown in Eagle's minimum essential medium supplemented with 10% fetal bovine serum (Biochrom AG, S0615), non-essential amino acids, 2 mM L-glutamine, and 1% streptomycin-penicillin (Sigma, P4333). Subconfluent cells were

transfected with plasmids using TransIT-LT1 (Mirus, MIR2300) following the supplier's instructions. Twenty-four hours after transfection cells were fixed and permeabilized 4% Paraformaldehyde for 10 minutes and washed two times in phosphate-buffered saline. Cells were then permeabilized using 0,1% Triton X-100 for 5 minutes, and then washed two times in phosphate-buffered saline. For blocking, the cells were incubated with 3% pre-immune goat serum in phosphate-buffered saline for 30 min at room temperature. Then incubated for 1 h at room temperature with the FK2 antibody diluted 1:1000 in PBS with 1% goat serum. Cells were then washed 7x in phosphate-buffered saline before the immunostaining for 1 h at room temperature using an Alexa-conjugated goat anti-mouse IgG secondary antibody (Molecular Probes) diluted 1:1000 supplemented with 1% goat serum. Before imaging cells were washed 7x in phosphate-buffered saline.

Leptomycin B. Leptomycin B was purchased from Sigma (L2913), diluted in methanol to a working concentration of 100 uM and used at a working concentration of 100 nM.

Transfection. Subconfluent cells were transfected with plasmids using TransIT-LT1 (Mirus, MIR2300) following the supplier's instructions. Twenty-four hours after transfection cells were fixed in 4% paraformaldehyde and analyzed by confocal fluorescence microscopy. For the pRev1.4-GFP assay, images were taken of live cells.

Fluorescence confocal microscopy analysis. Cells were examined using a Zeiss Axio Observer.Z1 LSM780 CLSM system (Carl Zeiss Microscopy GmbH, Jena) with 100X NA1.4 plan-apochromat or 63X NA1.4 plan-apochromat objective, running ZEN 2012 (black edition) software. Quantifications were performed using the Volocity software (Perkin Elmer).

Table1. Plasmids used in this study

Vectors and constructs used in this study	
Gateway cloning vectors	
pENTR1A	Invitrogen
pENTR2B	Invitrogen
pENTR3C	Invitrogen
pDONR 207	Invitrogen
pDONR 221	Invitrogen
Other vectors	
pEGFP-C1	Clontech
pDEST EGFP-C1	(Lamark et al., 2003)
pRev1.4-GFP	(Henderson & Eleftheriou, 2000)
cDNA inserts and mutations*	
pRev1.4-GFP NBR1 (169-186) NES 1	G. Evjen
pRev1.4-GFP NBR1 (557-574) NES 2	G. Evjen
pRev1.4-GFP p62 (303-320) NES	S. Pankiv
pENTR NBR1 Δ1-332	T. Lamark
pDONR 221 NBR1 Δ1-483	Y.P. Abudu
pENTR NBR1sr2 Δ1-332 Δ 497-579	T. Lamark
pENTR NBR1sr Δ1-332 Δ574-684	M.S. Næss
pDONR 207 NBR1 Δ1-332 Δ686-760	M.S. Næss
pENTR NBR1 sr Δ1-332 Δ760-878	M.S. Næss
pENTR NBR1 sr2 Δ1-332 Δ877-966	M.S. Næss
pENTR NBR1 Δ1-332 Δ616-966	T. Lamark
pDEST EGFP NBR1 Δ1-332	M.S. Næss
pDEST EGFP NBR1 Δ1-483	M.S. Næss
pDEST EGFP NBR1 Δ1-332 L561A/S562A/F563A/L565E/L566WE	G. Evjen
pDEST EGFP NBR1 sr2 Δ1-332 Δ497-579	M.S. Næss
pDEST EGFP NBR1 sr Δ1-332 Δ574-684	M.S. Næss
pDEST NBR1 Δ1-332 Δ686-760	M.S. Næss
pDEST EGFP NBR1 sr Δ1-332 Δ760-878	M.S. Næss
pDEST EGFP NBR1 sr2 Δ1-332 Δ877-966	M.S. Næss
pDEST EGFP NBR1 Δ1-332 Δ616-966	M.S. Næss
pDEST EGFP NBR1 WT	C. Sletten
pDEST EGFP NBR1 D50R	J. Nunn
pDEST EGFP NBR1 Δ1-129	T. Lamark
pDEST EGFP NBR1 sr2 D50R Δ167-184	T. Lamark
pDEST EGFP NBR1 sr2 D50R Δ167-184 Δ494-584	G. Evjen
pDEST EGFP NBR1 sr2 Δ1-185	G. Evjen
pDEST EGFP NBR1 sr2 Δ1-206	G. Evjen
pDEST EGFP NBR1 sr2 Δ1-215	G. Evjen
pDEST EGFP NBR1 sr2 Δ1-246	G. Evjen
pDEST EGFP NBR1 sr Δ1-275	G. Evjen

pDEST EGFP NBR1 D50R Δ185-332	G. Evjen
pDEST EGFP NBR1 D50R Δ213-249	G. Evjen
pDEST EGFP NBR1 D50R Δ288-329	G. Evjen
pDEST EGFP NBR1 D50R Δ183-275	G. Evjen
pDEST EGFP NBR1 D50R Δ167-275	G. Evjen
pDEST EGFP NBR1 D50R Δ185-332 WF153/154AA	G. Evjen
pDEST EGFP NBR1 D50R Δ185-332 Δ164−166	G. Evjen
pDEST EGFP NBR1 Δ1-129 Δ183-758	G. Evjen
pDEST EGFP NBR1 Δ1-129 Δ183-758 WF153/154AA	G. Evjen
pDEST EGFP NBR1 Δ1-129 Δ183-758 Δ164-166	G. Evjen
pDEST EGFP NBR1 Δ1-206 Δ278-758	G. Evjen
pDEST EGFP NBR1 Δ1-206 Δ336-758	G. Evjen

*For simplicity some constructs are listed only in the pDEST vector.

Results

Part 1: Cytoplasmic localization of NBR1 depends on two nuclear export signals, a strong in the N-terminal region of NBR1 and a weaker overlapping with the Clathrin box and LIR2

The subcellular localization of proteins is commonly analyzed by immunofluorescence. When staining for p62, the staining pattern is predominantly resolved as small, punctuate structures in the cytoplasm (Fig. 4). However, upon treatment with LMB, the immunofluorescent signal shifts almost completely to the nucleus. This indicates that the nucleocytoplasmic shuttling of p62 is hampered, leading to nuclear accumulation of p62.

A similar staining pattern can be observed for NBR1. Immunofluorescent staining of NBR1 in HeLa cells grown in normal conditions shows a distinct punctuate distribution in the cytoplasm, displaying partial overlap with p62 (Fig. 4). Upon LMB treatment, a substantial amount of larger NBR1-containing structures appears in the nucleus, which partially co-localize with p62 (Fig. 4). This indicates that NBR1 exhibits nuclear shuttling.

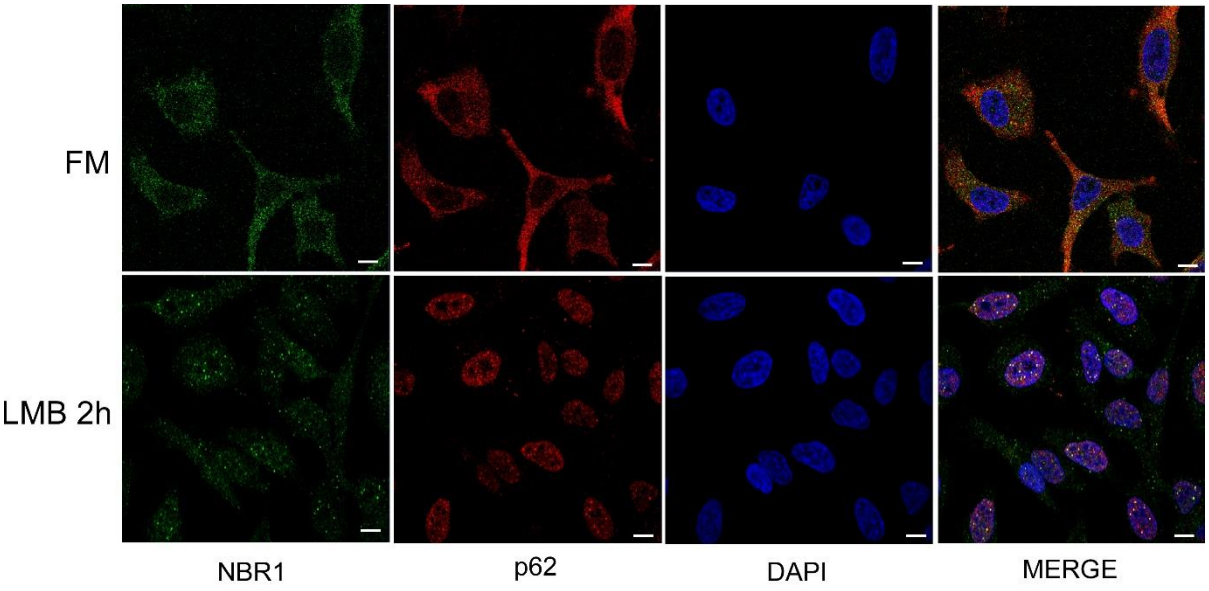

Figure 4. Endogenous p62 and NBR1 localize to the nucleus after LMB treatment. Representative immunofluorescence images of endogenous NBR1 (green) and p62 (blue). Under normal conditions, p62 and NBR1 reside in small cytoplasmic punctuate structures, with little or no nuclear presence. Upon inhibition of nuclear export by LMB, both p62 and NBR1 show translocalization to the nucleus. Scale bar 10 μm.

Since NBR1and p62 are binding partners and often found in the same cellular structures, it would be possible that the nuclear translocation of NBR1 is indirectly caused by binding to p62. It could also mean that NBR1 has its own NLS and NES sequences. Initially, we therefore set out to identify NES and NLS sequences in the C-terminal part of NBR1, but we deferred the quest for NLS due to its complexity. A sequence search for NES candidates identified different motifs depending on source [24]. Combining the web-based NES prediction servers NetNES (http://www.cbs.dtu.dk/services/NetNES/) and ELM (http://elm.eu.org/links.html) generated two mutual motifs that we named NES 1 (N-terminal) and NES2 (C-terminal) (Fig. 5).

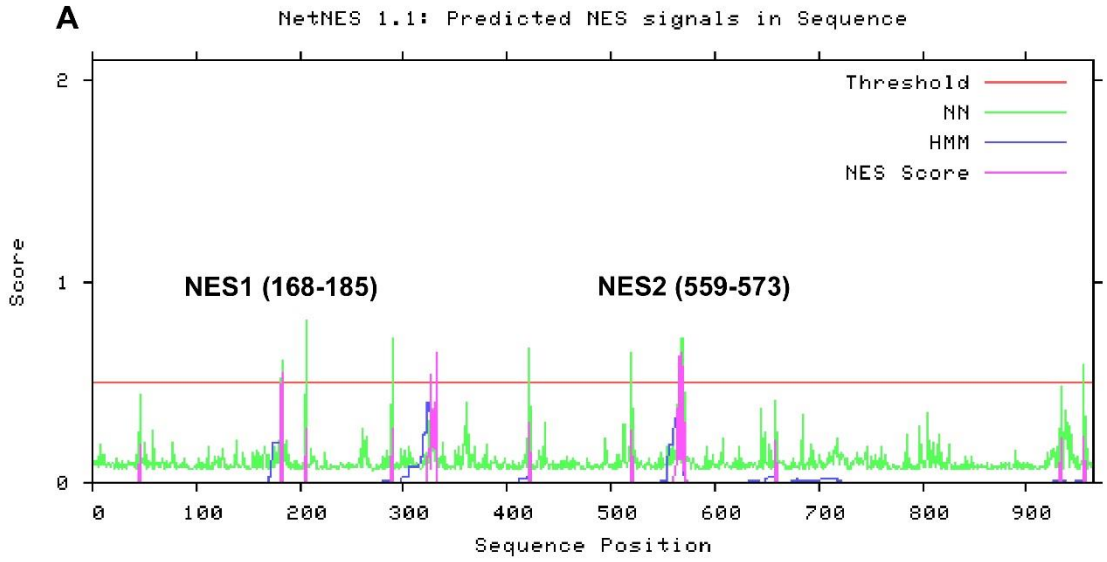

B

Consensus NES: Φ [L] x^{2-3} Φ [LIVFM] x^{2-3} Φ [LI] x Φ [LI]

REV1	**NES:**	**71**	**-**	**VPLQLPPLERLTLDCNE**	**-**	**87**
p62	**NES:**	**303**	**-**	**ATQSLAEQMRKIALESE**	**-**	**319**
NBR1	**NES 1:**	**168**	**-**	**TVEKLEQKLHEKLVLQN**	**-**	**185**
NBR1	**NES 2:**	**559**	**-**	**AQDLLSFELLDINIVQE**	**-**	**573**

Figure 5. Predicted NES sequences in NBR1. A) The combined sequence search for NES candidates in NBR1 identified two putative motifs. **B)** Sequence alignment of NES motifs from HIV1-REV1, p62 and the two identified motifs in NBR1. The NES consensus sequence is also shown. The amino acids that overlap with the important positions in the consensus sequence is highlighted in red.

Upon transient transfection, full length GFP-NBR1 is aggregated and cytoplasmic. LMB treatment does not induce a dominant nuclear accumulation of GFP-NBR1 WT (Fig. 6).

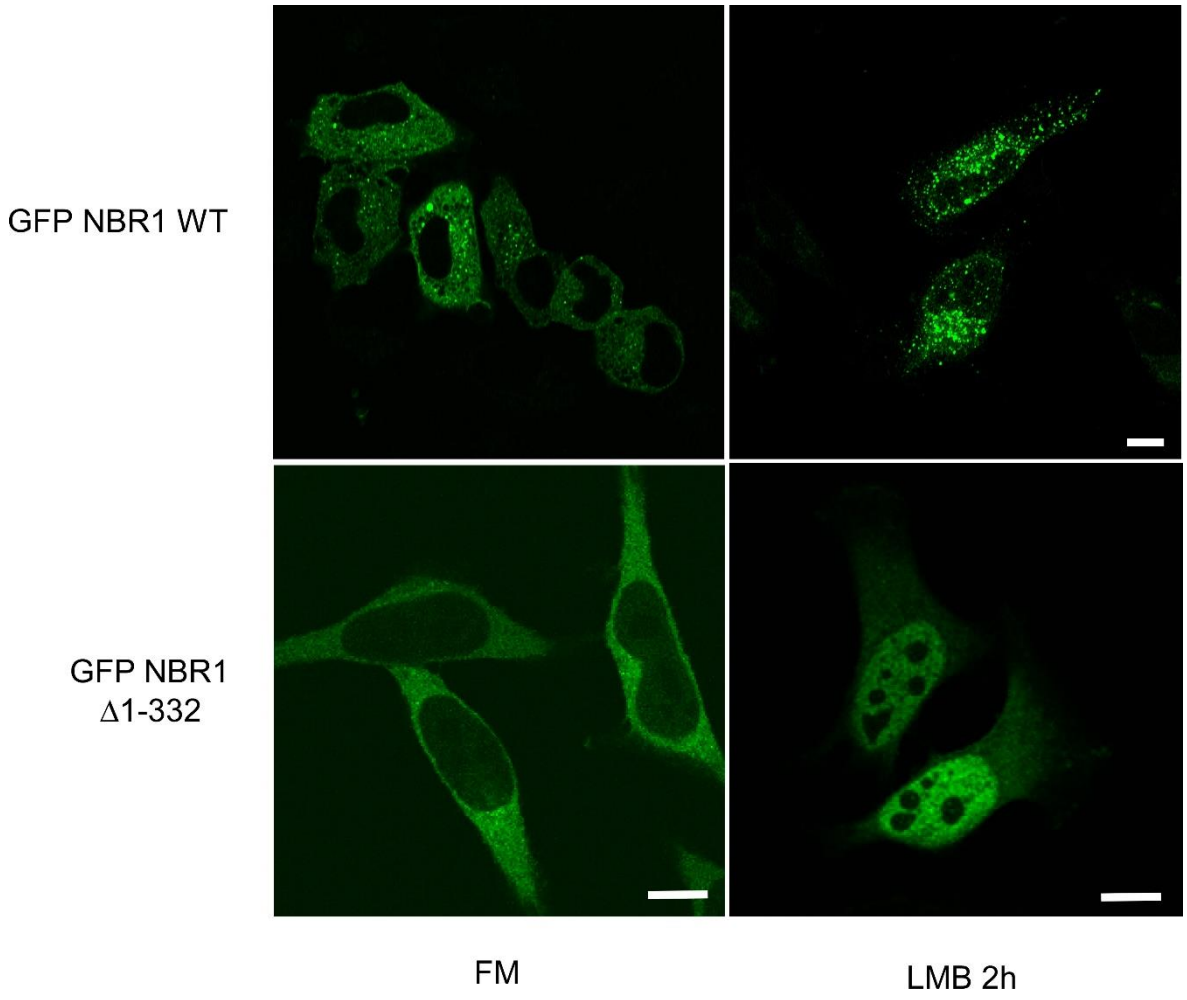

Figure 6. Cytosolic aggregation of NBR1 hampers nucleocytoplasmic shuttling. Overexpressed wild-type GFP-NBR1 is cytoplasmic and aggregated, and little nuclear localization is seen after 2h LMB treatment. N-terminally deleted NBR1 (amino acid 1-332) is also cytoplasmic, but diffuse, and is retained in the nucleus upon LMB treatment. Scale bar 10um.

Since full-length GFP-NBR1 is aggregated and cytoplasmic and does not clearly enter the nucleus with LMB treatment, the lack of nuclear import of overexpressed full-length NBR1 is presumably due to the extensive cytoplasmic aggregation phenotype (Fig. 6). A deletion of the N-terminal part of NBR1 encompassing amino acid 1-332 causes a complete loss of aggregation, and nucleocytoplasmic shuttling becomes apparent based on the shift from cytosolic to nuclear localization after LMB-treatment.

To verify the predicted NES-candidates, we started by making deletion constructs in the context of full-length NBR1. GFP-NBR1 D50R is also cytoplasmic, whereas constructs carrying NES1 deletions show some nuclear presence while those carrying NES2 deletions are entirely cytoplasmic. Deleting both NES-regions causes GFP-NBR1 to be predominantly nuclear (Fig. 7). Based on this we concluded that both NES-candidates contribute to the nuclear export of NBR1.

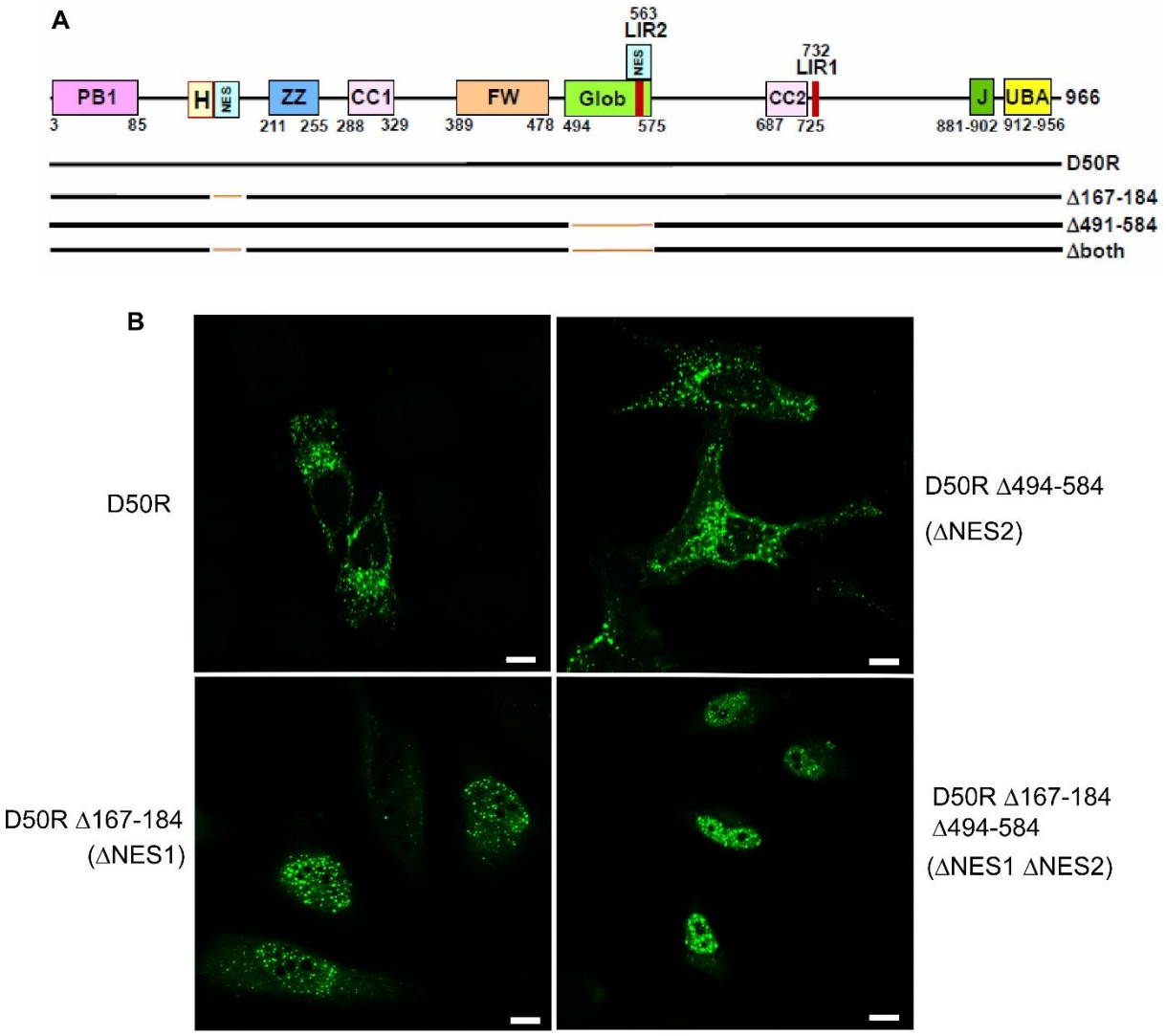

Figure 7. NBR1 has two functional NES motifs. A) Schematic representation of the NBR1-constructs used in B). **B)** Exogenously expressed GFP-NBR1 D50 with deletions in the two predicted NES regions. Full-length NBR1 resides mostly in the cytoplasm. A small deletion containing NES1 leads to a significant amount of nuclear retainment, whereas the larger deletion of GLOB2 (containing NES2) has little effect on subcellular distribution. With a combined deletion of both NES-regions, NBR1 shifts to an almost complete nuclear localization. Scale bar 10um

To further verify the NES candidates, we continued by cloning NES1 and NES2 into the pRev1.4-GFP assay system, placing the putative NES between the nuclear bound Rev protein from HIV and GFP. The control plasmid contains the REV1 protein sequence with a mutated NES-sequence, which leads to nuclear accumulation of the empty control vector (Fig. 8 and 9) [25]. To reverse nuclear aggregation the inserted NES has to compete out the active NLS in the Rev1-protein. As a control we used the p62 NES (303-320), which is known to be a very potent NES [26]. The ratio of Rev proteins outside versus inside the nucleus was quantified to evaluate the strength of each NES. These experiments were carried out in both HeLa cells (Fig. 8) and HEK293 cells (Fig. 9).

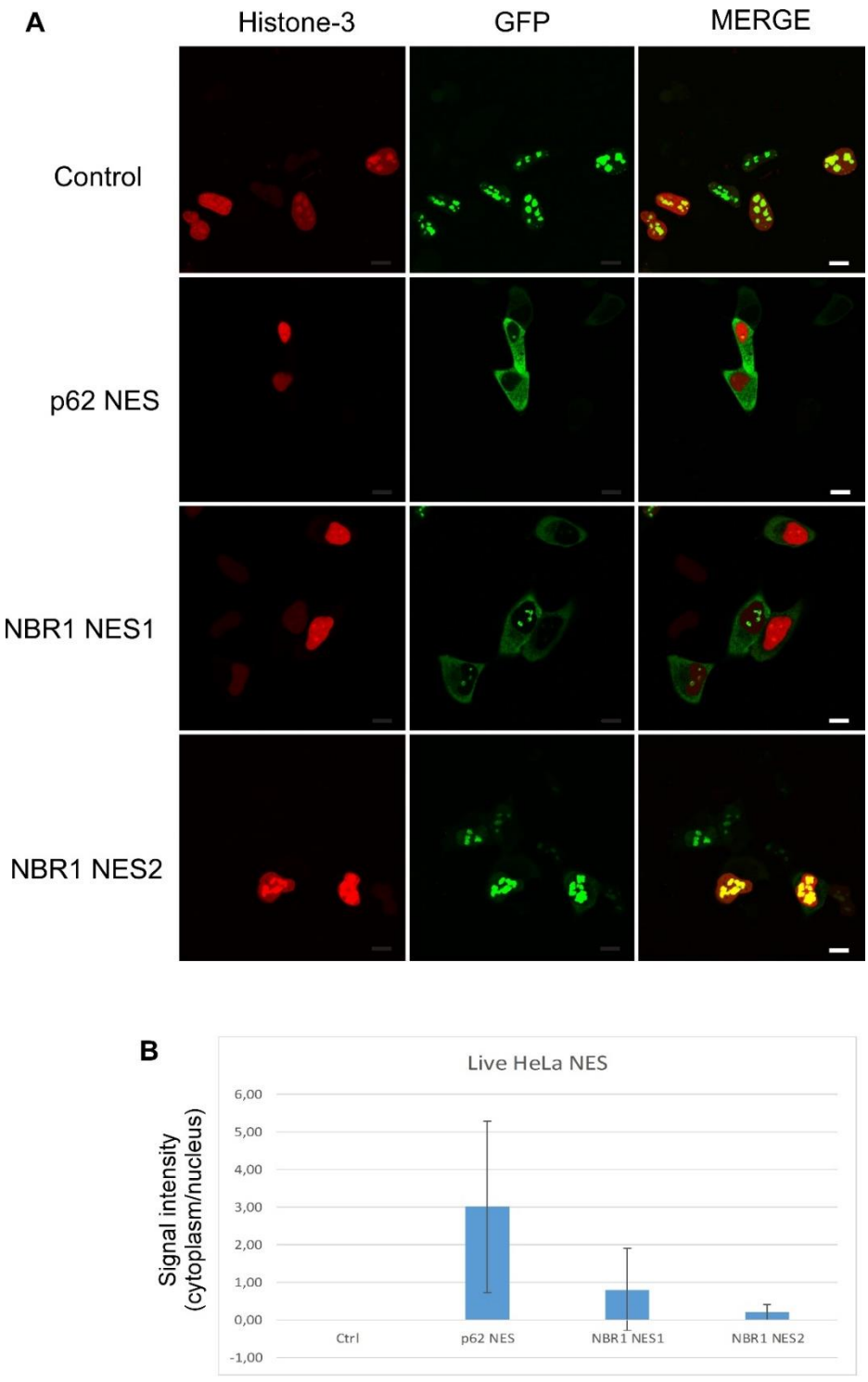

Figure 8. NBR1 contains two active NES-sequences. A) HeLa cells transiently expressing Rev-GFP, alone or fused to NES sequences from p62 and NBR1. Histone H3 was expressed with a mCherry-tag to visualize the nucleus. **B)** Quantification of the ratio of cytoplasmic and nuclear GFP signal, performed by separating the GFP signal from the nucleus and cytoplasm by colocalization with mCherry-Histone3. Imaging was carried out on live cells. Scale bar 10um.

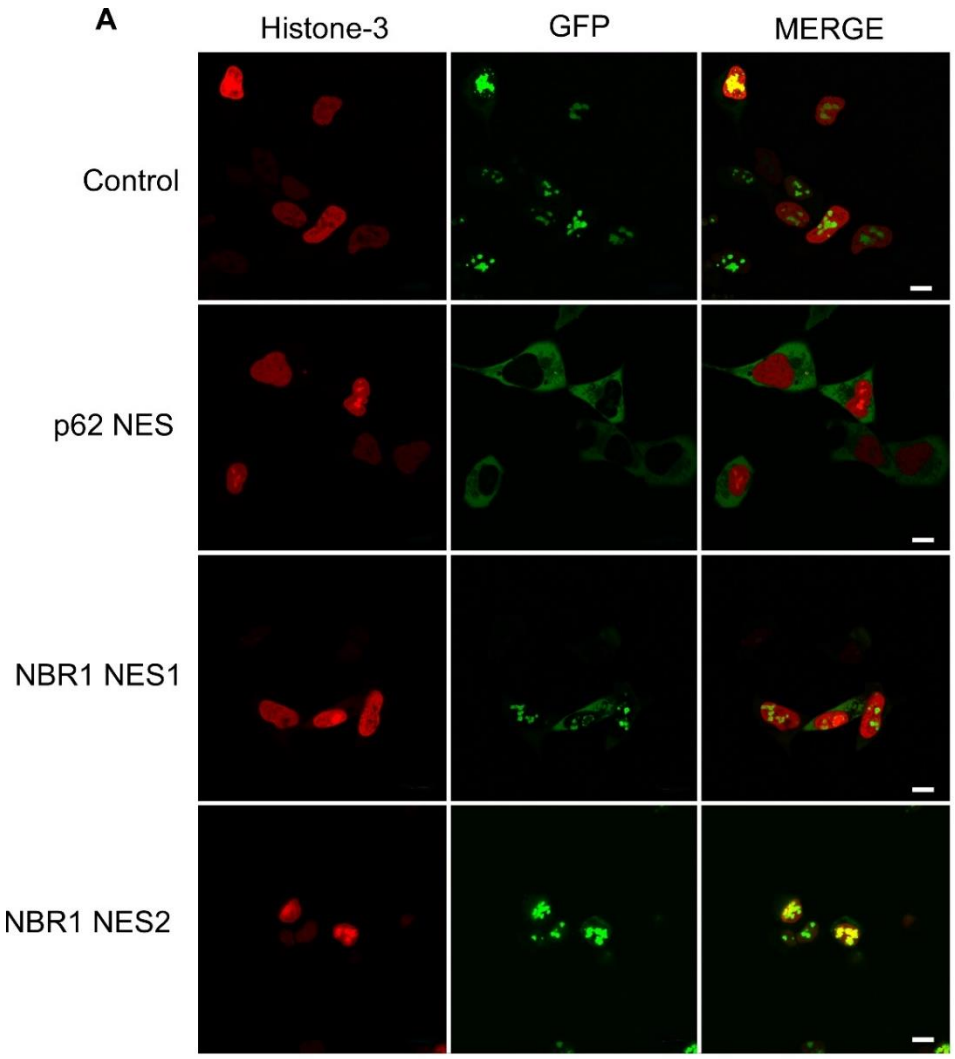

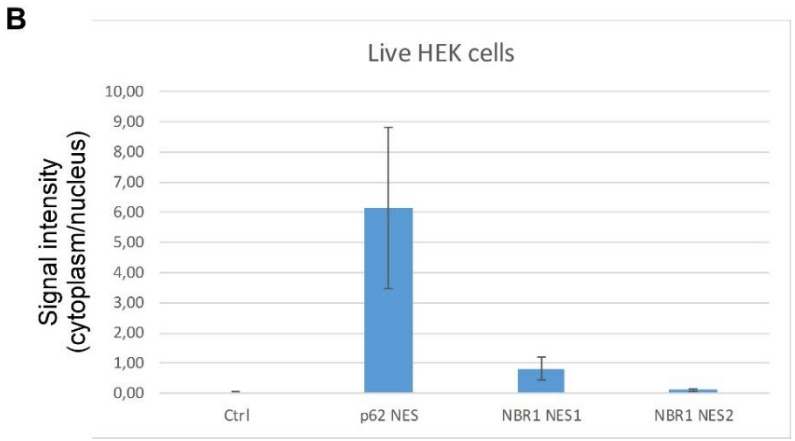

Figure 9. NBR1 contains two active NES-sequences. A) HEK cells transiently expressing Rev-GFP, alone or fused to NES sequences from p62 and NBR1. Histone3 was expressed with a mCherry-tag to visualize the nucleus. **B)** Quantification of the ratio of cytoplasmic and nuclear GFP signal, performed by separating the GFP signal from the nucleus and cytoplasm by colocalization with mCherry-Histone3. Imaging was carried out on live cells. Scale bar 10um.

The p62 NES is clearly strongest in both cell lines, and completely abrogates the nuclear import mediated by Rev1-NLS. The NES1 motif from NBR1 also gives increased cytoplasmic localization, whereas NBR1 NES2 is by far weakest. In conclusion, all three NES' facilitates nuclear export to a varying degree (Fig. 8 and 9). After two hours of LMB treatment, all Rev proteins were nuclear (data not shown).

To further validate the NES2 sequence from NBR1 we used the N-terminal GFP-NBR1 deletion construct Δ1-332, which shows complete diffuse and cytoplasmic localization (Fig. 10). Mutation or deletion of NES2 in NBR1 Δ1-332, lead to increased nuclear localization (Figure 10). This validates the function NES2 motif, despite the low export seen when using the Rev1.4. system.

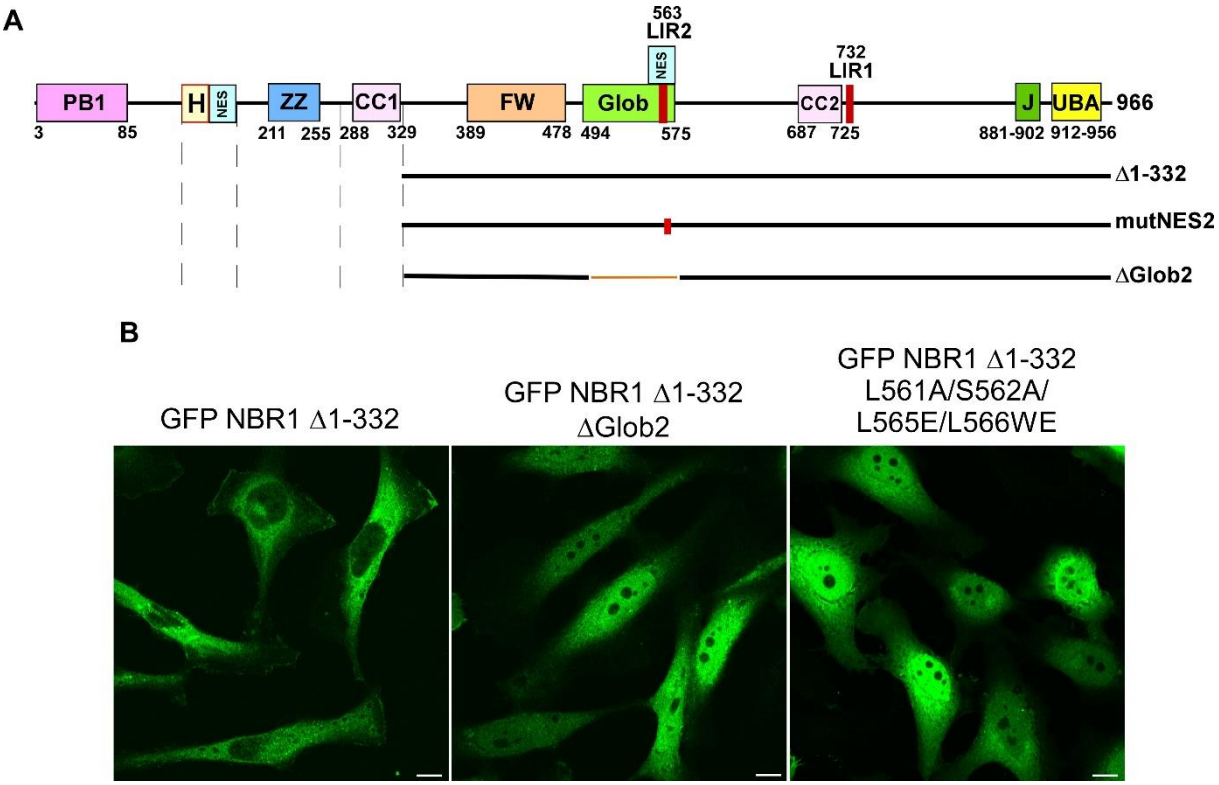

Figure 10. The Glob2 domain contains an active NES A) Schematic representation of NBR1 constructs used in B. **B)** GFP-NBR1 constructs ectopically expressed in HeLa cells. NBR1 lacking the first 332 amino acids localizes mainly to the cytoplasm. Upon deleting of the Glob2 domain, or mutating key residues in the predicted NES2-motif, the distribution becomes markedly more nuclear. Scale bar 10um.

GFP-NBR1 Δ1-332 ΔGlob2 has a more nuclear localization pattern, similar to the GFP-NBR1 Δ1-332 L561A/S562A/F563A/L565E/L566WE (Fig. 10). However, some cytoplasmic staining remains, and to rule out the possibility that other C-terminal regions beyond NES2 also could have possible effects on the nuclear export, we proceeded by making a series of deletion constructs targeting these regions in NBR1 Δ1-332 (Fig.11).

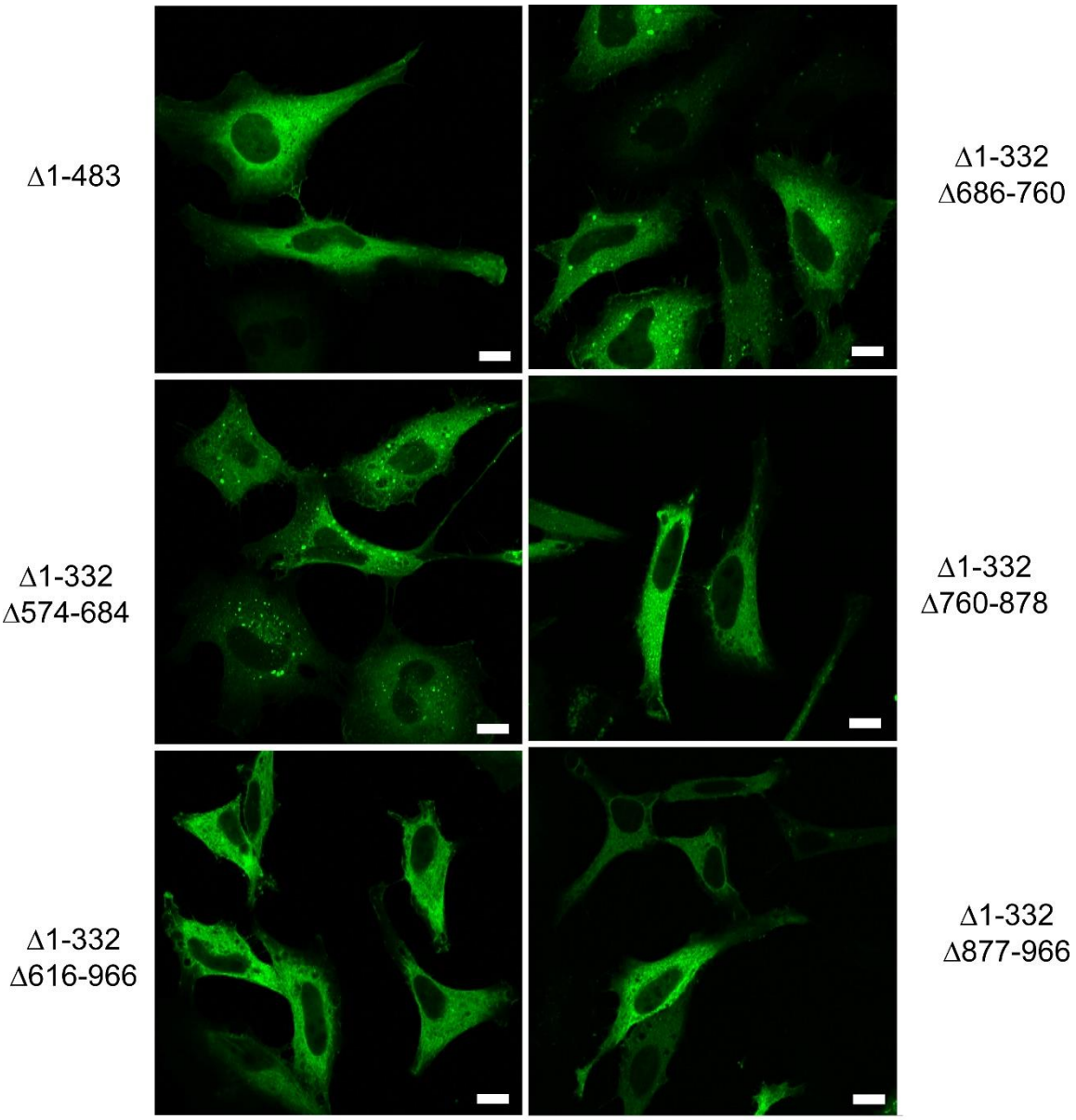

Figure 11. The NES2 is exclusive in NBR1 Δ1-332. GFP-NBR1 constructs ectopically expressed in HeLa cells. NBR1 lacking the first 332 amino acids localizes mainly to the cytoplasm. Scale bar 10um.

None of the constructs lacking NES1 with additional C-terminal deletions, but containing NES2, displayed a diminished ability to exit the nucleus (Fig. 11). These results indicate that C-terminal regions beyond NES2 have no additional effects on nuclear export.

Part 2: Aggregation strongly affects subcellular localization of N-terminally deleted NBR1 constructs.

Nuclear import or export of a given protein not only depends on its import or export signals, but also on interactions it may have with other cellular components. Overexpressed full-length NBR1 accumulates in large aggregates consisting of clusters of 50 nm vesicles [19], and we believe that this is the reason why we see no nuclear import of overexpressed NBR1 in response to a treatment with LMB (Fig. 6). The N-terminal part of NBR1 is required for aggregation of NBR1 (Fig.6). This was verified using stably expressing GFP-NBR1 FlpIn HEK 293 cells (Fig.12).

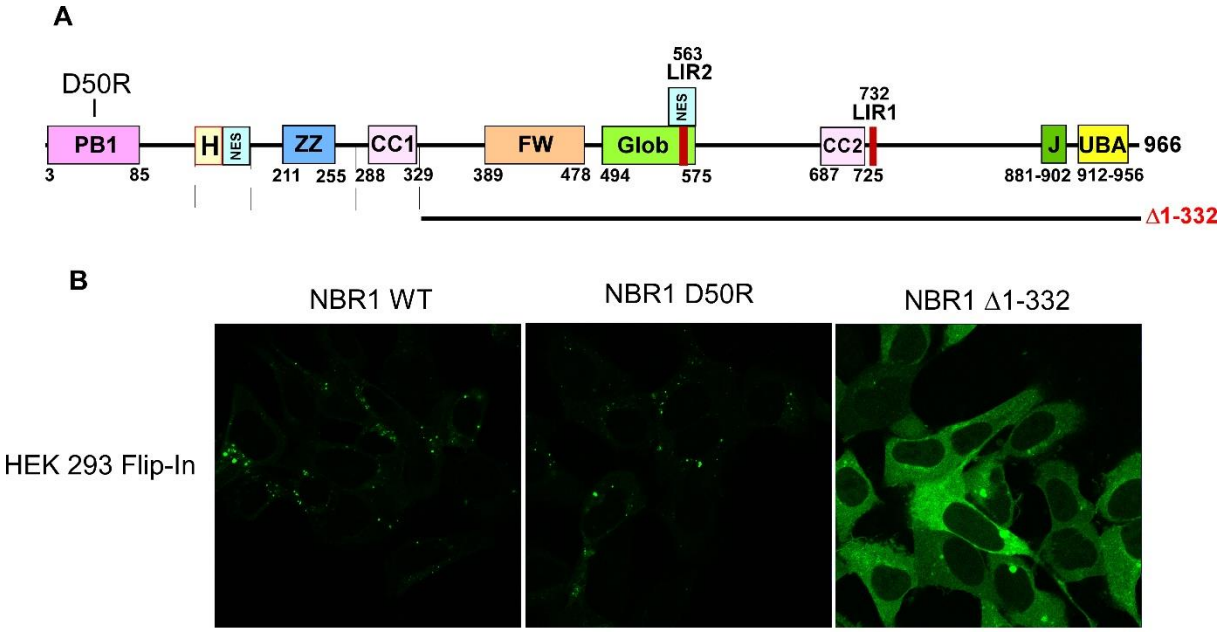

Figure 12. Stably expressed NBR1 requires the N-terminal region to form cytoplasmic aggregates. **A)** Schematic representation of NBR1 constructs used in B. **B)** Full-length NBR1 (both WT and D50R) forms cytosolic aggregates when stably expressed. Upon deletion of the N-terminal region encompassing amino acid 1-332 the cytosolic distribution of NBR1 is almost completely diffuse. Scale bar 10um.

To identify the specific region in the N-terminal part of NBR1 that is required for the aggregation of NBR1 in the cytoplasm, a series of deletion constructs of GFP-NBR1 were transiently transfected into HeLa cells and analyzed by confocal imaging (Fig. 13). Upon transient transfection, full-length GFP-NBR1 (WT) is cytoplasmic and aggregated, and GFP-NBR1 Δ1-129 lacking the PB1 domain has a similar localization pattern as GFP-NBR1 WT (Fig. 13). Both these constructs have NES1 and NES2 intact. The similar localization pattern of these two constructs indicates that the PB1 domain is not important for the aggregation of NBR1, and this is interesting since the PB1 of p62 is needed for aggregation of p62.

Subsequent extension of the N-terminal deletions of GFP-NBR1 (Δ1-185, Δ1-206, and Δ1-215) uphold aggregation, but the constructs become partially nuclear (Fig. 12). All these constructs are deleted for NES1 (aa 168-185), and their subcellular localization (Fig. 13) were highly similar to the localization pattern of GFP-NBR1 ΔNES1 (Fig. 7). All these deletion constructs were partially nuclear and formed both cytoplasmic aggregates and nuclear aggregates.

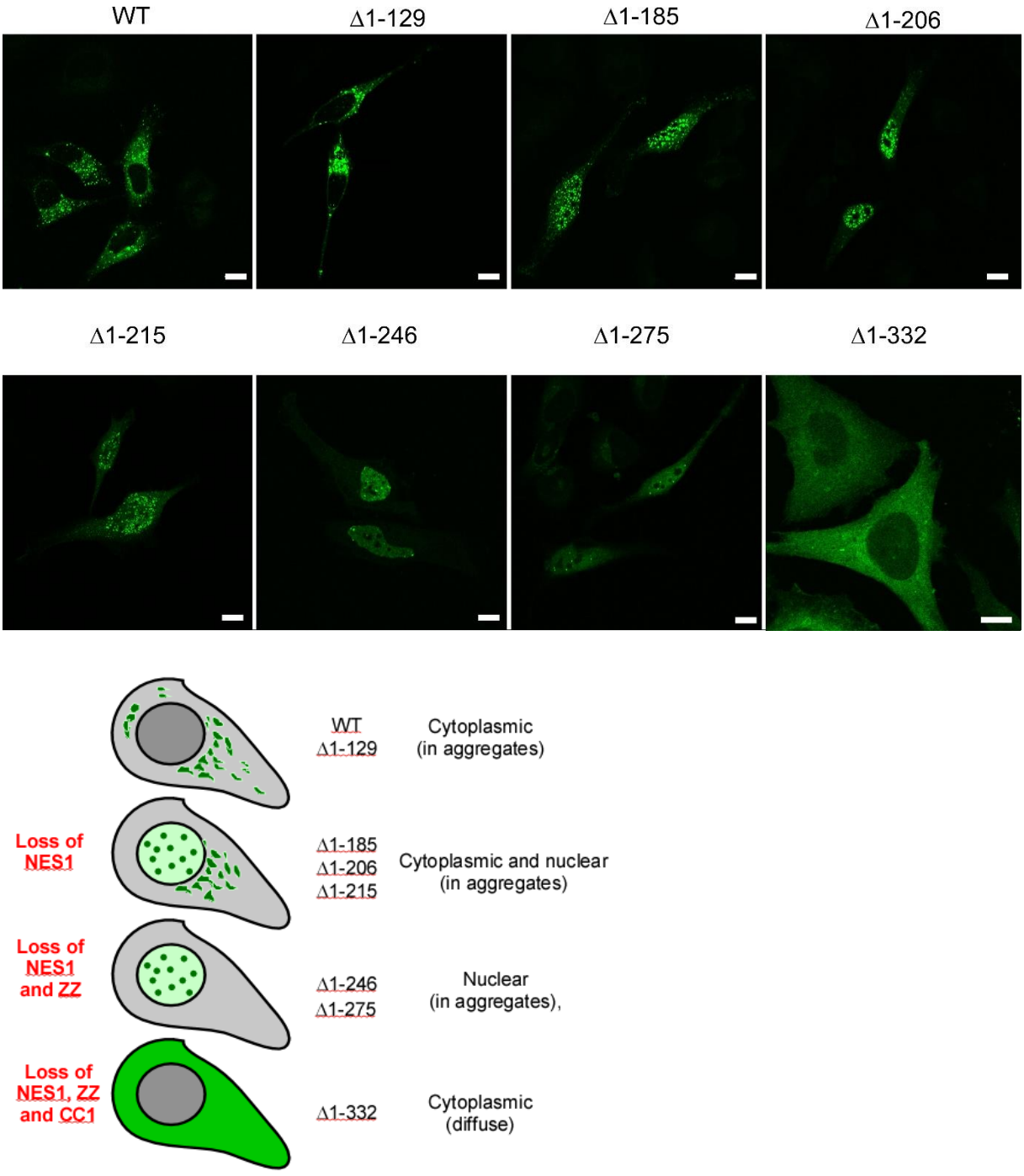

Figure 13. Aggregation effect on subcellular localization of N-terminally deleted NBR1 constructs. A) GFP-NBR1 constructs ectopically expressed in HeLa cells. Incremental deletions of the N-terminal region of NBR1. Full-length NBR1, as well as NBR1 lacking the N-terminal PB1-domain, both resides in cytoplasmic aggregates. When deletions include the NES1 motif, the subcellular localization turns nuclear and aggregated. Constructs lacking ZZ are also nuclear, but aggregates to a lesser extent and only in the nucleus. The deletion construct lacking NES1, ZZ and CC1 is more or less completely diffuse, and little or no nuclear localization can be seen. **B)** Illustration of the data shown in A. Scale bar 10um.

A further deletion of the Zinc finger domain (ZZ) strongly inhibited cytoplasmic aggregation of NBR1. The deletion constructs GFP-NBR1 Δ1-246 and GFP-NBR1 Δ1-275 both lack the ZZ domain, but they have CC1 intact. These constructs formed no cytoplasmic aggregates (Fig. 13), suggesting that the ZZ domain is required for cytoplasmic aggregation. However, these constructs did form nuclear aggregates (Fig. 13), suggesting that ZZ is not required for nuclear aggregation. Finally, these two constructs had a more nuclear localization than other transfected constructs, and in particular GFP-NBR1 Δ1-246 had a highly nuclear localization (Fig. 13). The lack of cytoplasmic aggregates, combined with the presence of nuclear aggregates, probably explain why these two constructs are so nuclear. Any nuclear aggregation is likely to have a negative effect on nuclear export.

Additional deletion of CC1, in GFP-NBR1 Δ1-332, produced a diffuse localization pattern with an almost complete loss of nuclear localization (Fig. 13). GFP-NBR1 Δ1-332 is recruited to the nucleus in response to treatment with LMB (Fig. 7) and it is completely diffuse also when in the nucleus. The cytoplasmic localization is probably mediated by the combined loss of nuclear aggregation, and the efforts of NES2. The finding that CC1 is needed for efficient nuclear aggregation of NBR1 is kind of expected since CC1 is responsible for oligomerization of NBR1 [27]. A role for oligomerization in aggregation is always very likely. From the data in figure 12, it cannot be excluded that CC1 is similarly required for aggregation of NBR1 in the cytoplasm. What was observed is that loss of ZZ prevented the formation of cytoplasmic aggregates, but it is possible that ZZ and CC1 are both required. For the aggregation of NBR1 in the cytoplasm, it is not known if ZZ and CC1 acts as individual domains, or if these two domains cooperate. It is also a possibility that CC1 is most important, but ZZ required because it is needed for the stabilization of ZZ. The loss of cytoplasmic aggregation is possibly mediated by an unfolding of NBR1 as Zinc-finger like domains stabilize proteins [28].

Aggregation of NBR1 in the nucleus does not depend on the ZZ domain, but the region between ZZ and CC1 may be important. GFP-NBR1 Δ1-246 and GFP-NBR1 Δ1-275 both contain the CC1 domain, but has the ZZ domain deleted. The only difference between these two constructs is that the region between ZZ and CC1 is deleted in GFP-NBR1 Δ1-275, but included in GFP-NBR1 Δ1-246. When overexpressed in HeLa cells, GFP-NBR1 Δ1-275 seemed to form less nuclear aggregates than GFP-NBR1 Δ1-246 and it was less nuclear. The longer deletion possibly causes a partial loss of CC1 function resulting in less nuclear aggregation due to reduced self-interaction.

Part 3: The ZZ-CC1 region and a conserved region preliminary named H-box can both nucleate aggregation of cytoplasmic NBR1

Since GFP-NBR1 Δ1-185 and Δ167-184 (ΔNES1) form aggregates (Fig. 13 and 7), while Δ1-332 is diffuse, we hypothesized that ZZ, CC1, or the region between ZZ and CC1, is required for cytoplasmic aggregation of NBR1. However, neither a specific deletion of CC1 (Δ288-329), ZZ (Δ213-249), nor the deletion encompassing both ZZ and the intermediate region between ZZ and CC1 (Δ183-275) affect aggregation of NBR1 after transient transfection in HeLa cells (Fig. 13). Even the larger deletion of GFP-NBR1 Δ185-332 does not remove aggregation (Fig. 14). This was a surprise, since it means that GFP-NBR1 Δ1-185 and GFP-NBR1 Δ185-332 can both form cytoplasmic aggregates. Since GFP-NBR1 Δ1-332 is diffuse and cytoplasmic, we believe there is more than a single region mediating cytoplasmic aggregation of NBR1.

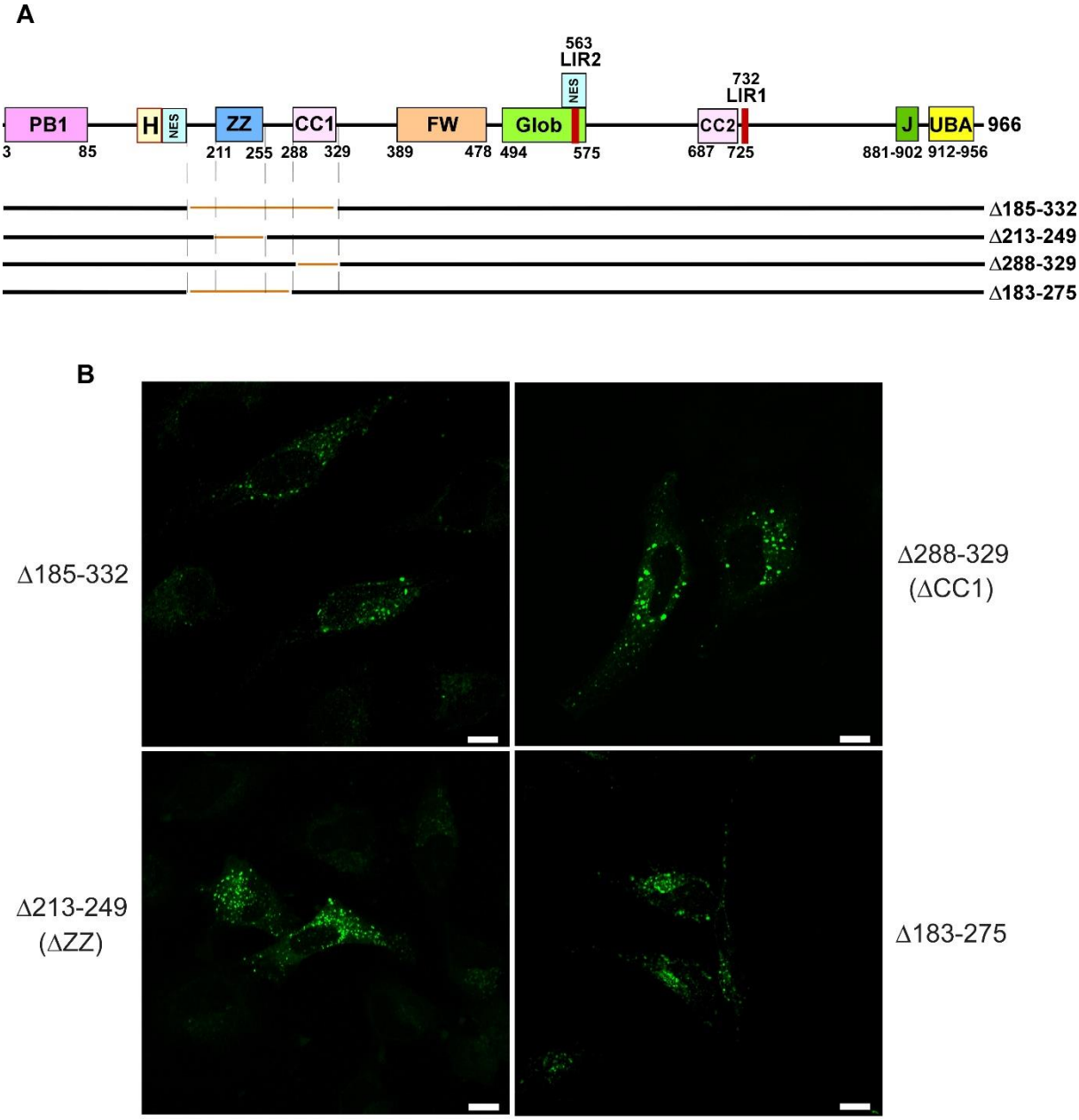

Figure 14. The Zinc-finger and Coiled-coil 1 domain is dispensable for NBR1 aggregate formation. **A)** Schematic representation of NBR1 constructs used in B. **B)** GFP-NBR1 D50R constructs ectopically expressed in HeLa cells. Deletion of regions containing the Zinc-finger and coiled coil domains, as well as the region between these two domains, does not alter NBR1s ability to form cytoplasmic aggregates. Scale bar 10 um.

When analyzing the sequence of NBR1, we discovered that the sequence N-terminally adjacent to NES1 is highly conserved. This sequence, amino acids 151-173, was preliminary named the H-box. Our NES1 deletion construct, GFP-NBR1 D50R Δ167-184 lacks the C-terminal part of the H-box, and the H-box may therefore be affected by our NES1 deletion. GFP-NBR1 Δ167-

184, lacking the C-terminus of the H-box, NES1, the ZZ domain and the intermediate region between ZZ and CC1, is completely diffuse when transiently expressed (Fig. 15)

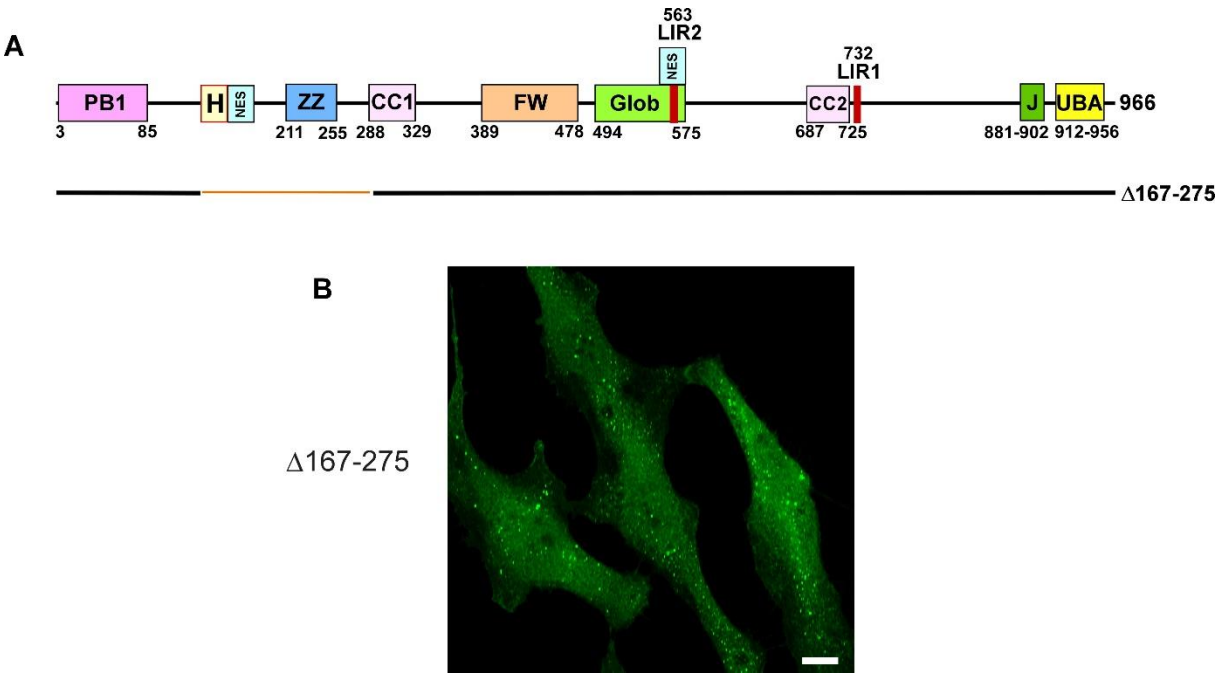

Figure 15. Deletion of the H-box prevents aggregation of NBR1 lacking ZZ and the intermediate region between ZZ and CC1 A) Schematic representation of NBR1 construct used in B. **B)** GFP-NBR1 D50R with a deletion ectopically expressed in HeLa cells. Deletion of the small region preceding the NES leads to a reduction in the aggregate forming potential of NBR1. Scale bar 10 um.

This sharply contrasts the aggregated localization pattern of GFP-NBR1 D50R Δ167-184 (Fig. 7) and NBR1 D50R Δ183-275 (Fig. 14), and strongly favors the assumption that the H-box and the ZZ-CC1 region are both independently capable of facilitating cytoplasmic aggregation of NBR1.

To verify that it was the mutation of the H-box, and not the deletion of NES1, that facilitated aggregation of NBR1, we made point mutations and deletions of specific amino acids within the conserved H-box in NBR1 D50R Δ185-332. We made two point mutations affecting two highly conserved amino acids s in the N-terminal part of the H-box (WF153/154AA), and one small deletion affecting three highly conserved residues in the middle of the H-box (Δ164-166) (Fig.16).

151 PDWFTSYLETFREQVVNETVEKL 173

Figure 16. Amino acid sequence of H-box in NBR1. Indicated in red are amino acids mutated in the WF153/154AA and Δ164-166 mutants. Underlined is the part of the H-box deleted in our NES1 deleted constructs (Δ167-184).

The WF153/154AA and Δ164-166 mutant constructs have NES1 intact but lacks the ZZ and CC1 domains. Their potential aggregation therefore depends on the H-box. Strikingly, both these constructs strongly inhibit the ability of GFP-NBR1 D50R Δ185-332 to aggregate (Fig. 17).

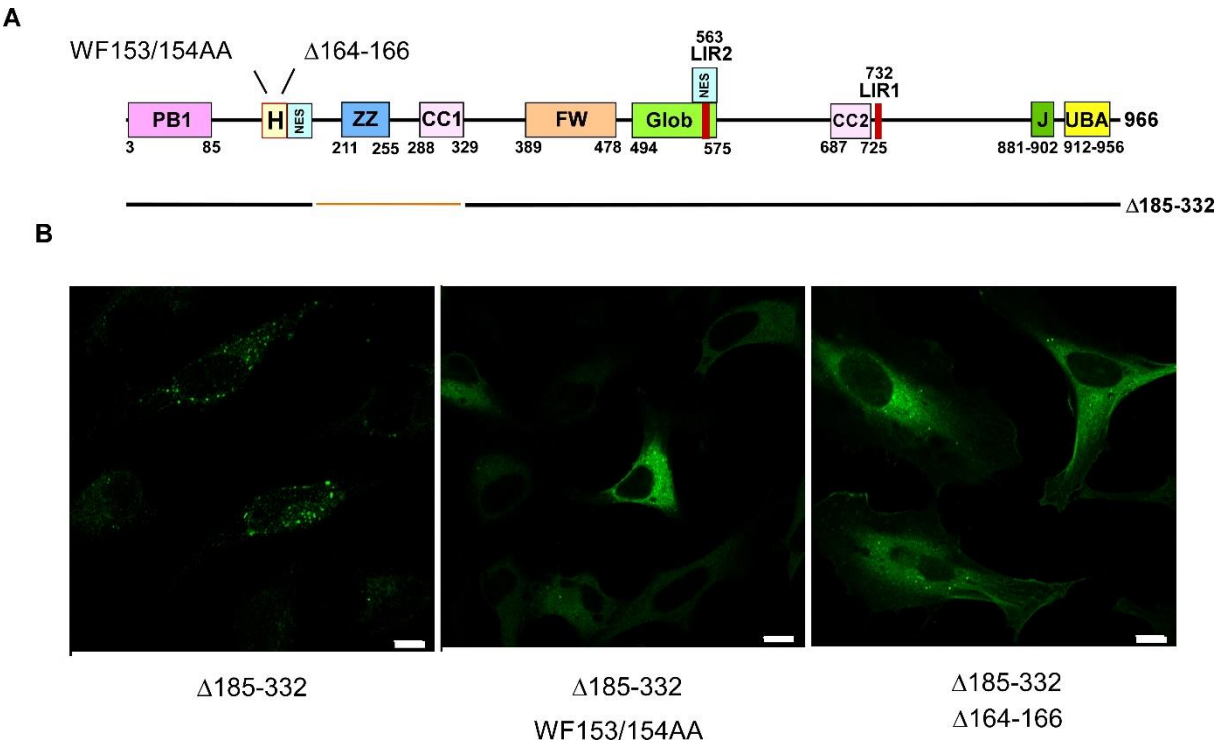

Figure 17. NBR1 Δ185-332 depends on H-box for aggregation A) Schematic representation of NBR1 construct used in B, including the indicated mutants. **B)** GFP-NBR1 D50R with indicated mutations and deletions ectopically expressed in HeLa cells. Mutation or deletion of conserved residues in the H-domain leads to a reduction in the aggregate forming potential of NBR1. Scale bar 10 um.

We conclude that NBR1 may use either the newly identified H-box or ZZ-CC1 to aggregate, and only if both these domains are deleted does NBR1 become diffuse (Fig. 17).

Part 4: Identifying the minimal NBR1 regions needed for aggregation

It is known from before that the amphipathic helix and UBA domain are needed for cytoplasmic aggregation of GFP-NBR1, but domains in the N-terminal part of NBR1 are additionally required. To further test if the H-box can induce aggregation of NBR1 in the absence of all other N-terminal domains of NBR1, a minimal construct was made: GFP-NBR1 Δ1-129 Δ183-758. In this construct, the H-box and NES1 (aa 130-182) is fused to a C-terminal fragment of NBR1 containing the amphipathic helix and UBA domain (Fig. 18). NES1 was included to prevent extensive nuclear accumulation. This construct was then tested for aggregation in transfected HeLa cells. GFP-NBR1 Δ1-129 Δ183-758 is highly cytoplasmic and it aggregates extensively (Fig.18). The H-box facilitates the cytoplasmic aggregation as point mutations in this region, WF153-154AA or Δ164-166, renders the construct diffuse with little or no aggregation (Fig. 17). Similar type of minimal constructs was also made where the ZZ domain (aa 207-277) or a larger piece containing both ZZ and CC1 (aa 207-335) were fused to the same C-terminal piece of NBR1 containing the amphipathic helix and UBA domain (Fig. 17). Both these H-box deleted constructs formed aggregates, but they accumulated in different compartments (Fig. 18). GFP-NBR1 Δ1-206 Δ278-758 lacks CC1, but contains ZZ and most of the internal region between ZZ and CC1. The protein is nuclear, cytoplasmic and quite diffuse, yet with cytoplasmic aggregates (Fig. 18). The cytoplasmic aggregation is interesting, since it indicates that ZZ does not absolutely depend on CC1 to induce aggregation. The lack of nuclear aggregates is expected since we show above that CC1 is needed for nuclear aggregation. GFP-NBR1 Δ1-206 Δ336-758 contain both ZZ and CC1. This construct forms primarily nuclear, but also some perinuclear aggregates (Fig. 18), and it is less diffuse than the construct lacking CC1.

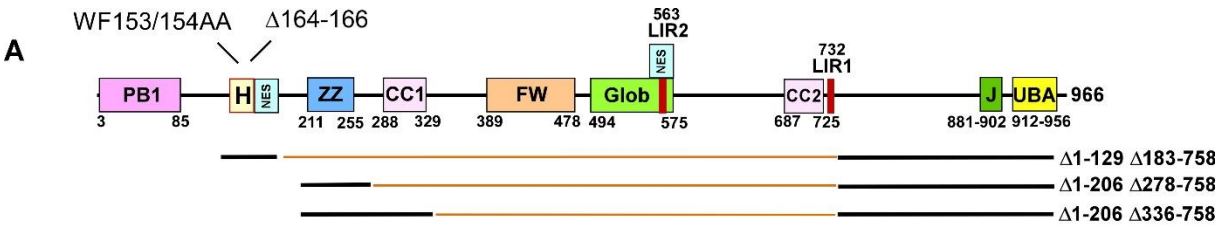
A
WF153/154AA
Δ164-166
563
LIR2
NES
732
LIR1
PB1
H
NES
ZZ
CC1
FW
Glob
CC2
J
UBA
966
3
85
211
255
288
329
389
478
494
575
687
725
881-902
912-956
Δ1-129 Δ183-758
Δ1-206 Δ278-758
Δ1-206 Δ336-758

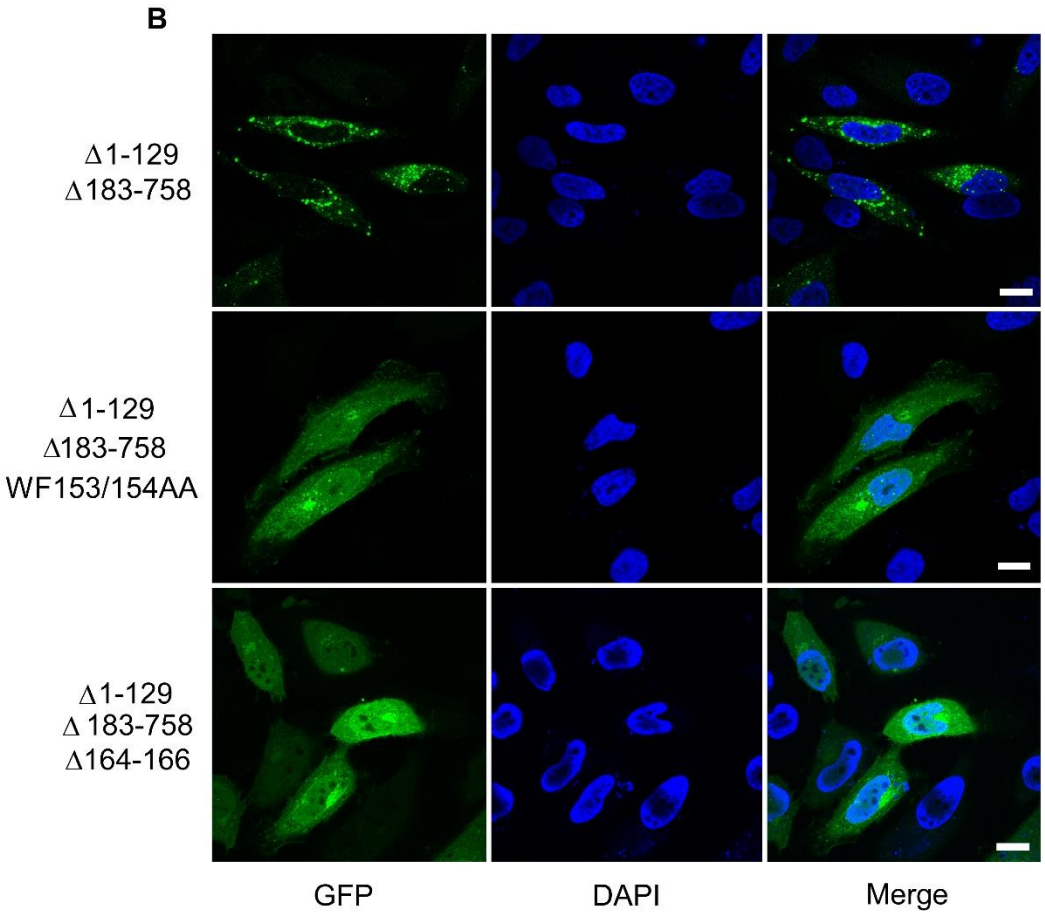
B
Δ1-129
Δ183-758
Δ1-129
Δ183-758
WF153/154AA
Δ1-129
Δ 183-758
Δ164-166
GFP
DAPI
Merge

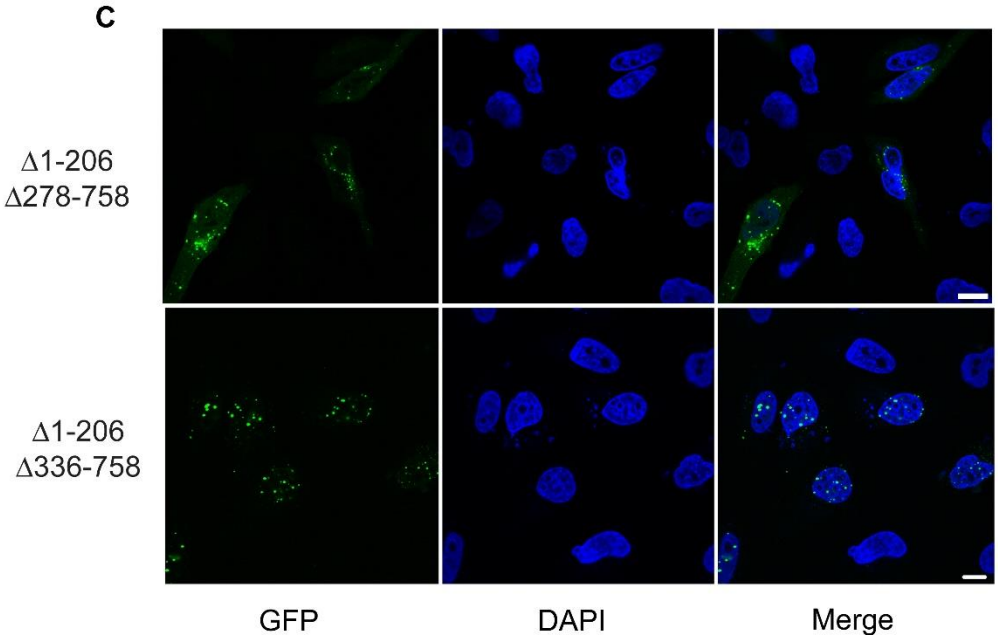
C
Δ1-206
Δ278-758
Δ1-206
Δ336-758
GFP
DAPI
Merge

Figure 18. NBR1 lacking the Zinc-finger and Coiled-coil domains depends on H-box for aggregation A) Schematic representation of NBR1 construct used in B and C, including the indicated mutants. **B)** GFP-NBR1 D50R with indicated mutations and deletions ectopically expressed in HeLa cells. Mutation or deletion of conserved residues in the H-domain leads to a reduction in the aggregate forming potential of NBR1. **C)** GFP-NBR1 D50R, minimal constructs containing either ZZ domain or both ZZ domain and CC1 fused to the C-terminal end of NBR1 expressing the amphipathic helix and UBA domains. Scale bar 10 um.

Discussion:

Our primary aim of this investigation was to map potential NES sequences in NBR1. The first step in this process was to find credible candidates, which we did by analyzing NBR1's amino acid sequence using two different web-based NES prediction servers, NetNES and ELM. The search identified two motifs that we named NES1 and NES2 (Fig. 5). In addition, a third putative NES sequence was identified in the CC1 domain (aa 288-329). Previous work in our group has shown the plasmid construct GFP-NBR1 275-333 to be nuclear in full medium [29]. This small construct may enter the nucleus either with or without an active NLS, but should at least be partly cytoplasmic with an active NES. As this construct is highly nuclear, an active NES in this region as predicted by NetNES, is unlikely. Thus, we focused our investigation on the two motifs shared by the two NES prediction servers. In one set of experiments, the cellular localization of NBR1 constructs deleted for one or both predicted NES motifs were analyzed by confocal imaging of transiently transfected cells. Loss of one NES had some effect on nuclear localization, but losing both NES motifs had a profound effect rendering the construct entirely nuclear (Fig. 7). As a second type of experiment, we used the pRev1.4-GFP assay system as this protein is completely nuclear. Adding NES1 or NES2 to this nuclear protein resulted in a partially cytoplasmic localization of the construct, and this verified the potential of these NES sequences to mediate nuclear export. In our assays, NES1 was shown to be the strongest NES in NBR1, but NES2 is likely to contribute to the nuclear export of NBR1. These experiments are all performed using transient transfection, and results may potentially have been different if the studied constructs were expressed in stable cell lines. However, this critique would be more pertinent if the experiments had other results, as overexpression most likely would lead to proteins staying in their subsequent compartments rather than translocating as a consequence of NES deletion (Fig. 7) or addition (Fig. 8 and 9), as was the case in these experiments. Thus, the conclusion that cytoplasmic localization of NBR1 depends on two NES, a strong in the N-terminal region of NBR1 and a weaker overlapping with the Clathrin box and LIR2 carries some weight. We believe NBR1 has two NES to make sure the protein is within the cytoplasm where it plays a role as an autophagy receptor together with p62 [11]. Our data from confocal microscopy show that both stable (Fig. 10) and transiently transfected (Fig. 6 and 7) full-length NBR1 is exclusively cytoplasmic. Deleting either single NES makes NBR1 less cytoplasmic and more nuclear, whereas deleting both NES1 and NES2 makes NBR1 predominantly nuclear (Fig. 7).

We do not yet know if NBR1 plays an important role in the nucleus, but as endogenous NBR1 shuttles between the cytoplasm and the nucleus (Fig. 4), we suspect NBR1 may play a similar role to p62 facilitating nuclear aggregation [21]. Endogenous p62 has a much more active rate of nuclear shuttling than NBR1, yet both of these proteins engage in nucleocytoplasmic shuttling. As there are no autophagosomes in the nucleus, p62 and NBR1 probably don't function as autophagy receptors within the nucleus, but as they bind to each other [12] these two proteins may have the same nuclear function. Our group have previously suggested the role of p62 in the nucleus to be "quality control" of proteins, although misfolded core proteins degrade in the proteasome and not in autophagosomes [21]. The assumption of "quality control is nurtured by the fact that p62 binds to the proteasome [30] , and we believe NBR1 may do the same. Since NBR1 accumulates in "punctuated structures" in the nucleus, an obvious thing to do in the future is to stain these dots with antibodies to see what they contain. If these dots contain p62 and even proteasomes, our suspicion that NBR1 plays an important role in the nucleus will be strengthened.

The second part of this paper was focused on finding N-terminal domains necessary for cytoplasmic aggregation of NBR1. Previous data show NBR1 accumulates in cytoplasmic vesicle-like clusters [31] depending on C-terminal amphipathic helix and UBA domain for cytoplasmic aggregation [19]. Our data introduce N-terminal domains necessary for cytoplasmic aggregation. First, while endogenous full-length NBR1 is aggregated and cytoplasmic, NBR1 Δ1-332 is diffuse and cytoplasmic demonstrating NBR1 require the N-terminal region to form cytoplasmic aggregates (Fig. 10). As both GFP-NBR1 Δ1-185 and GFP-NBR1 Δ185-332 form aggregates, there must be more than one region responsible for the ability to keep NBR1 diffuse and cytoplasmic, or at least two regions in the N-terminal of NBR1 with aggregation ability. (Fig. 13). The fact that more than one domain in the N-terminal region were capable of mediating cytoplasmic aggregation of NBR1 complicated matters.

Smaller N-terminal deletions were incrementally more cytoplasmic and aggregated, while larger N-terminal deletions were more nuclear and aggregated up to Δ1-246, after which constructs became gradually less nuclear and aggregated culminating in Δ1-332 being totally cytoplasmic and diffuse (Fig. 13). The incremental N-terminal deletions involved NES1, ZZ and CC1 to various degrees, and we sought to explain the different intracellular arrangements with the corresponding loss or presence of these domains. Surprisingly, both ZZ (aa 213-249) and CC1 (aa 288-329) are dispensable for NBR1 aggregate formation, meaning that NBR1 may form aggregates with either of these domains missing (Fig. 14).

A thorough analysis of NBR1 revealed that the sequence N-terminally adjacent to NES1, amino acids 151-173, is highly conserved. This sequence was preliminary named the H-box. The construct Δ183-275 lacks the ZZ domain, and it is cytoplasmic and aggregated (Fig. 14). However, mutation of the H-box renders this construct diffuse in the cytoplasm. The construct Δ167-275 lacks both the C-terminal part of the H-box and the ZZ domain, and this construct is also completely diffuse when transiently expressed (Fig. 15). This strongly suggests that the H-box provide NBR1 with aggregation ability. These findings are substantiated when minimal NBR1 constructs missing ZZ and CC1 domains depend on the H-box for aggregation (Fig. 18). In conclusion, NBR1 depends on either one of the N-terminal regions: the H-box or the ZZ-CC1 domains, plus the additional C-terminal amphipathic helix and UBA domain for cytoplasmic aggregation.

Cytoplasmic aggregation of full-length NBR1 presumably relies on all these domains. It remains to be tested if aggregates of NBR1 deleted for the H-box or the ZZ-CC1 domains have a different morphology than aggregates formed by full-length NBR1. The CC1 domain is essential for oligomerization of NBR1, and this domain was therefore expected to promote aggregation of NBR1. The need for the ZZ domain may indicate that it has a specific role associated with aggregation, but its presence may alternatively facilitate oligomerization in conjunction with the CC1 domain. The role of the H-box is not known, but its ability to promote aggregation of NBR1 may depend on an interaction with another protein. Future studies should therefore search for proteins interacting with the H-box. It will also be interesting to see whether the H-box is needed for autophagic degradation of NBR1, since aggregation is needed for selective autophagy [32].

References

1. Kaur, J. and J. Debnath, *Autophagy at the crossroads of catabolism and anabolism.* Nat Rev Mol Cell Biol, 2015. **16**(8): p. 461-472.
2. Mukherjee, A., et al., *Selective endosomal microautophagy is starvation-inducible in Drosophila.* Autophagy, 2016. **12**(11): p. 1984-1999.
3. Glick, D., S. Barth, and K.F. Macleod, *Autophagy: cellular and molecular mechanisms.* The Journal of pathology, 2010. **221**(1): p. 3-12.
4. Ohsumi, Y., *Historical landmarks of autophagy research.* Cell Res, 2014. **24**(1): p. 9-23.
5. Mizushima, N. and M. Komatsu, *Autophagy: Renovation of Cells and Tissues.* Cell, 2011. **147**(4): p. 728-741.
6. Rogov, V., et al., *Interactions between Autophagy Receptors and Ubiquitin-like Proteins Form the Molecular Basis for Selective Autophagy.* Molecular Cell, 2014. **53**(2): p. 167-178.
7. Bjorkoy, G., et al., *p62/SQSTM1 forms protein aggregates degraded by autophagy and has a protective effect on huntingtin-induced cell death.* J Cell Biol, 2005. **171**(4): p. 603-14.
8. Deretic, V., *Autophagy in Immunity and Cell-Autonomous Defense Against Intracellular Microbes.* Immunological reviews, 2011. **240**(1): p. 92-104.
9. Kirkin, V., et al., *A role for NBR1 in autophagosomal degradation of ubiquitinated substrates.* Mol Cell, 2009. **33**(4): p. 505-16.
10. Waters, S., et al., *Interactions with LC3 and polyubiquitin chains link nbr1 to autophagic protein turnover.* FEBS Lett, 2009. **583**(12): p. 1846-52.
11. Kirkin, V., et al., *NBR1 cooperates with p62 in selective autophagy of ubiquitinated targets.* Autophagy, 2009. **5**(5): p. 732-3.
12. Lamark, T., et al., *Interaction codes within the family of mammalian Phox and Bem1p domain-containing proteins.* Journal of Biological Chemistry, 2003. **278**(36): p. 34568-34581.
13. Kraft, C., M. Peter, and K. Hofmann, *Selective autophagy: ubiquitin-mediated recognition and beyond.* Nat Cell Biol, 2010. **12**(9): p. 836-41.
14. Svenning, S., et al., *Plant NBR1 is a selective autophagy substrate and a functional hybrid of the mammalian autophagic adapters NBR1 and p62/SQSTM1.* Autophagy, 2011. **7**(9): p. 993-1010.
15. Sugawara, K., et al., *The crystal structure of microtubule-associated protein light chain 3, a mammalian homologue of Saccharomyces cerevisiae Atg8.* Genes to Cells, 2004. **9**(7): p. 611-618.
16. Nunn, J.A.L., *Functional characterization and regulation of the selective autophagy receptor NBR1.* PhD thesis November 2014, 2014.
17. Kraft, C., M. Peter, and K. Hofmann, *Selective autophagy: ubiquitin-mediated recognition and beyond.* Nat Cell Biol, 2010. **12**(9): p. 836-841.
18. Mardakheh, Faraz K., et al., *Nbr1 Is a Novel Inhibitor of Ligand-Mediated Receptor Tyrosine Kinase Degradation*. Vol. 30. 2010. 5672-85.
19. Deosaran, E., et al., *NBR1 acts as an autophagy receptor for peroxisomes.* Journal of Cell Science, 2013. **126**(4): p. 939.
20. Nakano, Y., et al., *PML Nuclear Bodies Are Altered in Adult-Onset Neuronal Intranuclear Hyaline Inclusion Disease.* Journal of Neuropathology & Experimental Neurology, 2017. **76**(7): p. 585-594.
21. Pankiv, S., et al., *Nucleocytoplasmic Shuttling of p62/SQSTM1 and Its Role in Recruitment of Nuclear Polyubiquitinated Proteins to Promyelocytic Leukemia Bodies.* Journal of Biological Chemistry, 2010. **285**(8): p. 5941-5953.

22. Sloan, K.E., P.E. Gleizes, and M.T. Bohnsack, *Nucleocytoplasmic Transport of RNAs and RNA-Protein Complexes.* J Mol Biol, 2016. **428**(10 Pt A): p. 2040-59.
23. Hutten, S. and R.H. Kehlenbach, *CRM1-mediated nuclear export: to the pore and beyond.* Trends Cell Biol, 2007. **17**(4): p. 193-201.
24. García-Santisteban, I., S. Bañuelos, and Jose A. Rodríguez, *A global survey of CRM1-dependent nuclear export sequences in the human deubiquitinase family.* Biochemical Journal, 2012. **441**(1): p. 209-217.
25. Henderson, B.R. and A. Eleftheriou, *A Comparison of the Activity, Sequence Specificity, and CRM1-Dependence of Different Nuclear Export Signals.* Experimental Cell Research, 2000. **256**(1): p. 213-224.
26. Pankiv, S., et al., *p62/SQSTM1 binds directly to Atg8/LC3 to facilitate degradation of ubiquitinated protein aggregates by autophagy.* J Biol Chem, 2007. **282**(33): p. 24131-45.
27. Lamark, T., et al., *NBR1 and p62 as cargo receptors for selective autophagy of ubiquitinated targets.* Cell Cycle, 2009. **8**(13): p. 1986-90.
28. Perales-Calvo, J., A. Lezamiz, and S. Garcia-Manyes, *The Mechanochemistry of a Structural Zinc Finger.* J Phys Chem Lett, 2015. **6**(17): p. 3335-40.
29. Olsvik, H.L., *Mapping of functional domains in the autophagic cargo receptor NBR1*. 2009, UiT Arctic university of Tromsø.
30. Seibenhener, M.L., et al., *Sequestosome 1/p62 Is a Polyubiquitin Chain Binding Protein Involved in Ubiquitin Proteasome Degradation.* Molecular and Cellular Biology, 2004. **24**(18): p. 8055-8068.
31. Kirkin, V., et al., *A Role for NBR1 in Autophagosomal Degradation of Ubiquitinated Substrates.* Molecular Cell, 2009. **33**(4): p. 505-516.
32. Johansen, T. and T. Lamark, *Selective autophagy mediated by autophagic adapter proteins.* Autophagy, 2011. **7**(3): p. 279-96.